Investigation of Bunsen flame dynamics by the method of characteristics

Investigation of Bunsen flame dynamics by the method of characteristics

M.L. BONDAR ‡, R.M.M. MATTHEIJ AND J.H.M. TEN THIJE BOONKKAMP
Department of Mathematics and Computer Science, Eindhoven University of Technology,
PO Box 513, 5600 MB Eindhoven, The Netherlands

Abstract

Understanding the dynamics and the stabilisation of flames is important for practical applications and for theoretical research. Here, to investigate the time-evolution of a Bunsen flame in a Poiseuille flow, we extend a G-equation-based kinematic model by accounting for flame stabilisation. The nonlinear G-equation is solved analytically using the methods of characteristics. The solution is then used to assess the dynamics of the Bunsen flame reaching its stationary position. The stationary position is stable with respect to small perturbations of the flame front. The time required for stabilization is further characterized by employing a detailed analytical investigation.
Keywords: G-equation, method of characteristics, Bunsen flame, flame stabilisation, stabilisation time

1. Introduction

Understanding the dynamics of flames propagating from an initial kernel to the stationary position is of central interest in the study of combustion (Lewis & von Elbe (1961)). Due to computational costs, simulations of flame dynamics in its entire complexity (i.e., by accounting for the coupling between the gas flow, convection, and the ignition-induced chemical reactions) remain prohibitive. Analytical studies using simplified flame models allow for a qualitative understanding of the flame dynamics. To assess the evolution of the flame we use in this paper a kinematic model that is widely used in the field of acoustic instabilities (e.g. Fleifil *et al.* (1996); Dowling (1999); Ducruix *et al.* (2000); Lieuwen (2005)). In this model, the flame is reduced to an infinitely thin surface separating the burnt from the unburnt gas. The movement of this separating surface which is denoted here as the flame front is described by a kinematic relation known as the G-equation (Markstein (1964)). The flame front moves under the action of the flow velocity $\mathbf{v}$ and the laminar burning velocity $\mathbf{S}_\mathrm{L}$. The laminar burning velocity is normal to the flame front and directed towards the unburnt gas (Figure 1), and its modulus S_L which we refer to as the flame speed, is assumed constant. The gas at the tube exit is modelled, e.g., as a Poiseuille flow, and the thermal expansion across flame is neglected.

Because of these simplifying assumptions, when using the kinematic model, the flow velocity

‡corresponding author:mbondar@win.tue.nl

cannot equate the laminar burning velocity. Consequently, the flame does not reach a stationary position. While in the kinematic model the laminar burning speed is constant, in reality it balances the flow velocity. In addition the laminar burning velocity decreases near the burner rim due to heat losses, such that at the burner rim there is a region where $\mathbf{S}_\mathrm{L}$ vanishes (Lewis & von Elbe (1961)). In order to investigate the dynamics of the flame reaching its stationary position and the stabilization time we extend the kinematic model by introducing a mathematical rule that allows the flame to reach a stable position. By using this new model, the flame whose kernel is initially fully developed at the tube exit (i.e., at time $t = 0$) reaches a stationary position equal to the steady solution of the G-equation in finite time. The shape of the initial flame kernel is considered a disk with radius R equal to the tube radius. The stationary position is stable with respect to small perturbation in the flame front.

In the extended model presented here, the movement of the flame front from the initial ($t = 0$) to the stationary position is determined by solving the G-equation analytically. Due to the nonlinearity of the G-equation a general analytical solution for an arbitrary flow field cannot be obtained. In previous studies an approximate, linear form of the G-equation could be derived and solved for the case of flames nearly parallel to the stream lines i.e., flames with sharp tip angles Fleifil *et al.* (1996) and for flames with a constant laminar burning velocity, normal to a stationary position of the flame (Boyer & Quinard (1990); Ducruix *et al.* (2000)). The G-equation was also used to derive an equation for the slope at the flame front (which is a quasi-linear hyperbolic equation) that could be solved by using the method of characteristics (Lieuwen (2005)). Consequently, the the flame front is attached at the burner rim by imposing boundary conditions.

To avoid the restrictions imposed by the solution procedures described above we solve the (nonlinear) G-equation directly with the method of characteristics. By working with the nonlinear equation instead of a linearised form we address here flames that have arbitrary cone angles and a laminar burning velocity of constant modulus that does not have a constant direction to a stationary position of the flame front. Furthermore in contrast with the previous models in which the flame attachment is imposed in the approach discussed here the flame attachment is a natural consequence of the flame stabilisation.

One of the most important results is that we are able to give analytical expressions for the location of the flame front along the characteristics, for the location of the characteristics and for the stationary position of the flame front by using elliptic integrals. A detailed analysis of the stabilisation time indicates that the nondimensional stabilisation time is approximately one. The stabilisation time of the flame is proportional to the ratio between the tube radius and the laminar burning speed.

The paper is organised as follows. First, we introduce the G-equation (Section 2) and Charpit's equations for the G-equation (Section 3). In Section 4 we derive analytical expressions for the location of the characteristics and for the flame front along the characteristics in terms of elliptic integrals. These analytical expressions are then used to compute the location of the flame front, and the stabilization rule is derived (Section 5). A detailed analysis of the stabilization time is presented in Section 6. Finally, the stationary position of the flame front is proved to be stable with respect to the stabilisation procedure (Section 7) and the conclusions are discussed (Section 8).

2. The G-equation

In the G-equation model for flame dynamics, the flame front is defined as the set of points $\mathbf{x}$ satisfying the relation $G(\mathbf{x}, t) = G_0$ for some scalar function G and a relevant G_0. The flame front separates the burnt gas ($G(\mathbf{x}, t) > G_0$) from the unburnt gas ($G(\mathbf{x}, t) < G_0$). The velocity

of the flame front $\mathbf{v}_\mathrm{f}$, can be written as

$$\mathbf{v}_\mathrm{f} = \mathbf{v} + \mathbf{S}_\mathrm{L} = \mathbf{v} + \mathrm{S}_\mathrm{L}\mathbf{n}, \qquad \mathbf{n} = -\nabla G/|\nabla G|, \tag{2.1}$$

where $\mathbf{n}$ is the unit normal on the flame surface, directed towards the unburnt gas mixture (Figure 1).

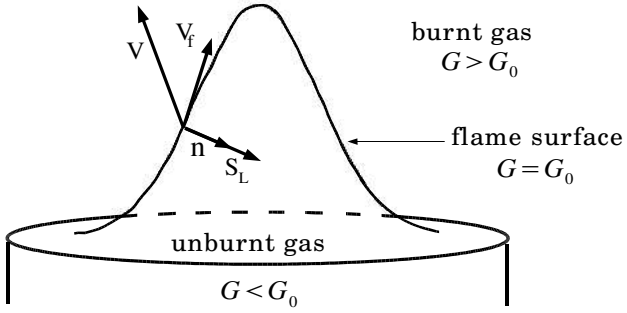

Figure 1: Flame front kinematics.

The motion of the flame front is described by the kinematic condition

$$\frac{\mathrm{d}G}{\mathrm{d}t} := \frac{\partial G}{\partial t} + (\mathbf{v}_\mathrm{f} \cdot \nabla)G = 0, \tag{2.2}$$

which means that a point on the flame front remains on the front for all time t. Substituting (2.1) in (2.2), the so-called G-equation is obtained

$$\frac{\partial G}{\partial t} + \mathbf{v} \cdot \nabla G = S_L|\nabla G|. \tag{2.3}$$

Since the flow has an axisymmetric profile the flame can be considered axisymmetric as well. This reduces the geometry to a two dimensional domain. Then the surface of the flame can be described by the relation $G(r, t, z) = G_0$ where r and z are the radial and axial coordinates, respectively. Since the flame is not locally vertical we can apply the implicit function theorem to express z as a function of the other two variables, i.e. $z = \zeta(r, t)$. Consequently, the relation

$$G(r, z, t) = z - \zeta(r, t), \tag{2.4}$$

determines the flame surface. Substituting (2.4) in (2.3), the following equation for the location of the flame front is obtained

$$\frac{\partial \zeta(r,t)}{\partial t} + u\frac{\partial \zeta(r,t)}{\partial r} - v + S_L\sqrt{\left(\frac{\partial \zeta(r,t)}{\partial r}\right)^2 + 1} = 0, \tag{2.5}$$

where u and v are the radial and axial components of the gas velocity, respectively. To find the location of the flame front, equation (2.5) needs to be solved.

3. Charpit's equations for the G-equation

Introducing the variable $q := \partial\zeta/\partial t$ we obtain the following expression for (2.5)

$$F(r, t, \zeta, p, q) := q + up - v + S_\mathrm{L}\sqrt{p^2 + 1} = 0. \tag{3.1}$$

Equation (3.1) is a nonlinear, first order PDE that can be solved analytically by using the method of characteristics (Kevorkian (1990)) for "simple" expressions for u, v and S_L. The solution is obtained by smoothly joining all the characteristic strips that emerge from the noncharacteristic initial strip defined by the initial condition $\zeta(r,0) = z_0(r)$, $p(r,0) = z_0'(r)$. This reduces (3.1) to a system of five ODEs, so-called Charpit's equations.

Charpit's equations for (3.1) for a general flow field $u(r,z,t)$ and $v(r,z,t)$ are given below. Let us introduce a parameter s along the characteristics and a parameter σ along the initial curve $t = 0$. In the following the notation $a(s;\sigma)$ is used for a generic variable a to indicate that an expression only holds along a characteristic parametrized by s. The parameter σ indicates that the characteristic passes through the point $(0,\sigma)$. The notation $a(r,t)$ is used in the case where an expression holds in the $(r,t)-$ plane. Assuming a constant speed S_L, Charpit's equations and the initial conditions for a general flow field $u(r,z,t)$ and $v(r,z,t)$ for equation (3.1) become

$$\frac{\mathrm{d}r}{\mathrm{d}s} = u + S_\mathrm{L}\frac{p}{\sqrt{p^2+1}}, \qquad r(0;\sigma) = \sigma, \tag{3.2a}$$

$$\frac{\mathrm{d}t}{\mathrm{d}s} = 1, \qquad t(0;\sigma) = 0, \tag{3.2b}$$

$$\frac{\mathrm{d}\zeta}{\mathrm{d}s} = p\left(u + S_\mathrm{L}\frac{p}{\sqrt{p^2+1}}\right) + q, \qquad \zeta(0;\sigma) = z_0(\sigma), \tag{3.2c}$$

$$\frac{\mathrm{d}p}{\mathrm{d}s} = -\left[p\frac{\partial u}{\partial r} - \frac{\partial v}{\partial r} + p\left(p\frac{\partial u}{\partial z} - \frac{\partial v}{\partial z}\right)\right], \qquad p(0;\sigma) = z_0'(\sigma), \tag{3.2d}$$

$$\frac{\mathrm{d}q}{\mathrm{d}s} = -\left[p\frac{\partial u}{\partial t} - \frac{\partial v}{\partial t} + q\left(p\frac{\partial u}{\partial z} - \frac{\partial v}{\partial z}\right)\right], \qquad q(0;\sigma) = q_0(\sigma). \tag{3.2e}$$

Note that $q(s;\sigma)$ can be eliminated from (3.2c) using (3.1) and that the initial condition $q_0(\sigma)$ follows from the other initial conditions. From (3.2b) we simply obtain $t(s;\sigma) = s$, and it remains for us to solve (3.2a), (3.2c) and (3.2d). The system reduces to

$$\frac{\mathrm{d}r}{\mathrm{d}t} = u + S_\mathrm{L}\frac{p}{\sqrt{p^2+1}}, \qquad r(0;\sigma) = \sigma, \tag{3.3a}$$

$$\frac{\mathrm{d}\zeta}{\mathrm{d}t} = v - S_\mathrm{L}\frac{1}{\sqrt{p^2+1}} \qquad \zeta(0;\sigma) = z_0(\sigma), \tag{3.3b}$$

$$\frac{\mathrm{d}p}{\mathrm{d}t} = -p\frac{\partial u}{\partial r} + \frac{\partial v}{\partial r} - p\left(p\frac{\partial u}{\partial z} - \frac{\partial v}{\partial z}\right), \qquad p(0;\sigma) = z_0'(\sigma). \tag{3.3c}$$

Charpit's equations (3.3) for a Poiseuille flow are solved in the next section.

4. Solution for a Poiseuille flow

Since the axial component of the velocity is dominant except near the base of the flame (Lieuwen (2003)) the gas flow at the tube exit as well as inside the tube is approximated by a Poiseuille

flow described by

$$u(r) = 0, \qquad v(r) = v_0\left(1 - \left(\frac{r}{R}\right)^2\right), \tag{4.1}$$

where v_0, u, v denote the maximum velocity of the flow, the radial and the axial components of the gas velocity, respectively. The variables in (3.3) are scaled as follows

$$r^* := r/R, \quad t^* := t/\hat{t}, \quad \sigma^* := \sigma/R, \quad \zeta^* := \zeta/R, \tag{4.2}$$

where $\hat{t} := R/S_{\mathrm{L}}$. The dimensionless system (omitting the $*$) corresponding to equation (3.1) is

$$\frac{\mathrm{d}r}{\mathrm{d}t} = \frac{p}{\sqrt{p^2+1}}, \qquad r(0;\sigma) = \sigma, \tag{4.3a}$$

$$\frac{\mathrm{d}\zeta}{\mathrm{d}t} = \hat{v}(1-r^2) - \frac{1}{\sqrt{p^2+1}}, \qquad \zeta(0;\sigma) = z_0(\sigma), \tag{4.3b}$$

$$\frac{\mathrm{d}p}{\mathrm{d}t} = -2\hat{v}r, \qquad p(0;\sigma) = z_0'(\sigma), \tag{4.3c}$$

where $\hat{v} := v_0/S_{\mathrm{L}}$ is typically in the interval $\hat{v} \in [2, 10]$. The formal solution procedure for the system (4.3) is as follows. First, we find the expression for $p(r;\sigma)$. Second, we determine the location of the characteristics in an implicit form $t = t(r;\sigma)$ and find the location of the flame front $\zeta(r;\sigma)$ along the characteristics. Third, we invert the implicit relation $t = t(r;\sigma)$, to find $\sigma = \sigma(r,t)$ and replace σ in the expression for $\zeta(r;\sigma)$ to find the position $\zeta(r,t)$ of the flame front.

To start with, from (4.3a) and (4.3c) the following differential equation is obtained

$$\frac{p}{\sqrt{p^2+1}}\mathrm{d}p = -2\hat{v}r\mathrm{d}r. \tag{4.4}$$

Since $p \le 0$, we obtain by integrating (4.4)

$$p(r;\sigma) = -\sqrt{\left(c(\sigma) - \hat{v}r^2\right)^2 - 1}, \tag{4.5}$$

where $c(\sigma) := \sqrt{1 + z_0'(\sigma)^2} + \hat{v}\sigma^2 \ge 1$. Second, using (4.5) in (4.3a) and applying the corresponding initial condition the integral form of the location of the characteristics is obtained, i.e.,

$$t(r;\sigma) = -\int_\sigma^r \frac{c(\sigma) - \hat{v}x^2}{\sqrt{\left(c(\sigma) - \hat{v}x^2\right)^2 - 1}}\,\mathrm{d}x. \tag{4.6}$$

The integral at the right hand side term of (4.6) cannot be evaluated analytically. However, it is possible to reformulate (4.6) in terms of elliptic integrals of first and second kind (Abramowitz & Stegun (1974); Byrd & Friedman (1971)). For $0 \le m \le 1$ and $0 \le \phi \le \pi/2$ the functions

$$F(\phi, m) := \int_0^\phi \frac{1}{\sqrt{1 - m^2\sin^2 x}}\,\mathrm{d}x, \quad E(\phi, m) := \int_0^\phi \sqrt{1 - m^2\sin^2 x}\,\mathrm{d}x, \tag{4.7}$$

are the elliptic integrals of the first and second kind, respectively. The number m is the *modulus* and the variable integration limit ϕ is the *argument* of the elliptic integral. When $\phi = \pi/2$ the elliptic integrals are said to be *complete* and they are denoted by

$$F(\pi/2, m) := K(m), \quad E(\pi/2, m) := E(m), \tag{4.8}$$

respectively. The values for elliptic integrals can be taken from tables (Abramowitz & Stegun (1974); Byrd & Friedman (1971)) or computed with an algorithm by Carlson & Notis (1981) based on the paper by Carlson (1979). To simplify the expressions for $t(r;\sigma)$ and $\zeta(r;\sigma)$ that follow, we introduce the auxiliary variables

$$k(\sigma) := \sqrt{\frac{c(\sigma)-1}{c(\sigma)+1}}, \quad \psi(r;\sigma) := \arcsin\left(r\sqrt{\frac{\hat{v}}{c(\sigma)-1}}\right), \quad \tau(\sigma) := \psi(\sigma;\sigma), \tag{4.9a}$$

$$\mathcal{E}(\psi,\tau,k) := E(\psi,k) - E(\tau,k), \quad \mathcal{F}(\psi,\tau,k) := F(\psi,k) - F(\tau,k). \tag{4.9b}$$

With these variables (4.6) becomes

$$t(r;\sigma) = \frac{1}{\sqrt{\hat{v}(c(\sigma)+1)}}\mathcal{F}(\psi,\tau,k) - \sqrt{\frac{c(\sigma)+1}{\hat{v}}}\mathcal{E}(\psi,\tau,k). \tag{4.10}$$

Combining (4.3a) and (4.3b) we obtain

$$\frac{\mathrm{d}\zeta}{\mathrm{d}r} = \frac{\hat{v}(1-r^2)\sqrt{p^2+1}-1}{p}. \tag{4.11}$$

Integrating (4.11) and using and (4.5) and (4.6) we obtain the following integral expression for the location of the flame front along the characteristics

$$\zeta(r;\sigma) = z_0(\sigma) + \hat{v}t(r;\sigma) + \int_\sigma^r \frac{1+\hat{v}x^2(c(\sigma)-\hat{v}x^2)}{\sqrt{\left(c(\sigma)-\hat{v}x^2\right)^2-1}}\,\mathrm{d}x. \tag{4.12}$$

After elaborate calculations the integral relation (4.12) can be written in terms of elliptic integrals. Using the notations in (4.9), we obtain the following expression for $\zeta(r;\sigma)$,

$$\begin{aligned}\zeta(r;\sigma) &= z_0(\sigma) + \hat{v}t(r;\sigma) + \left(\frac{c(\sigma)\sqrt{c(\sigma)+1}}{3\sqrt{\hat{v}}}\right)\mathcal{E}(\psi,\tau,k) + \\ &\left(\frac{2-c(\sigma)}{3\sqrt{\hat{v}(c(\sigma)+1)}}\right)\mathcal{F}(\psi,\tau,k) - \\ &\frac{1}{3}\left(r\sqrt{(c(\sigma)-\hat{v}r^2)^2-1} - \sigma\sqrt{(c(\sigma)-\hat{v}\sigma^2)^2-1}\right).\end{aligned} \tag{4.13}$$

Third, to find the location of the flame front $\zeta(r,t)$, σ as a function of r and t is needed which can be found using (4.6), or equivalently (4.10). This is possible only if

$$J(r;\sigma) := \frac{\partial t(r;\sigma)}{\partial \sigma} \neq 0. \tag{4.14}$$

Because of the complicated formula in (4.10), it is difficult to investigate the sign of $J(r;\sigma)$ for a general initial profile of the flame front. However, we are interested in studying the movement of the flame front for the special case $z_0(r) = 0$. Then the variables $k(\sigma)$, $\psi(r;\sigma)$ and $\tau(\sigma)$ reduce to

$$k(\sigma) = \sqrt{\frac{\hat{v}\sigma^2}{\hat{v}\sigma^2+2}}, \quad \psi(r;\sigma) = \arcsin\left(\frac{r}{\sigma}\right), \quad \tau(\sigma) = \frac{\pi}{2}. \tag{4.15}$$

With these notations the Jacobian (4.14) for $z_0(r) = 0$ becomes

$$\begin{aligned}J(r;\sigma) &= \frac{1}{\sigma\sqrt{\hat{v}(\hat{v}\sigma^2+2)}}\Bigg(\mathcal{F}(\psi,\tau,k) - (\hat{v}\sigma^2+1)\mathcal{E}(\psi,\tau,k) + \\ &\frac{r\hat{v}(\sigma^2-r^2)(\hat{v}\sigma^2+1)+r(\hat{v}\sigma^2+2)}{\sqrt{(\sigma^2-r^2)(\hat{v}\sigma^2+2)(\hat{v}(\sigma^2-r^2)+2)}}\Bigg).\end{aligned} \tag{4.16}$$

For $0 < r < \sigma$ we have $J(r;\sigma) > 0$, which makes it possible to use the implicit function theorem and therefore to determine σ as a function of r and t.

5. Flame stabilisation

The flame moves under the influence of the Poiseuille flow and of the laminar burning velocity whose speed is constant. At the edge of the tube a region exists where the laminar burning velocity is larger than the gas velocity and the flame is pushed into the tube. To overcome this unrealistic behaviour of the modelled flame, we improve the kinematic model by assuming that S_{L} is constant only in the region where the gas velocity is larger than the laminar burning velocity, i.e. $0 \le r \le \delta$, where δ is such that $\hat{v}(1-\delta^2) = 1$. This gives

$$\delta = \sqrt{1 - \hat{v}^{-1}}. \tag{5.1}$$

In the sequel we will refer to $0 \le r \le \delta$ as the *physical domain*.

Because it is not possible to invert (4.10) analytically we use the following numerical approach. A uniform grid is introduced for the space and time domains, i.e. $r_j = j\Delta r$, $j = 1, \ldots, M$, $t^n = n\Delta t$, $n = 0, \ldots, N$, with the grid size $\Delta r = \delta/M$ and time step $\Delta t = 1/N$. For given r_j and t^n we compute the corresponding σ_j^n from (4.6) using the secant method. From the geometrical viewpoint this means that at a certain moment in time t^n we trace back along the characteristic which passes through r_j, and we find the intersection point σ_j^n of the characteristic with the initial line $t = 0$ (Figure 2).

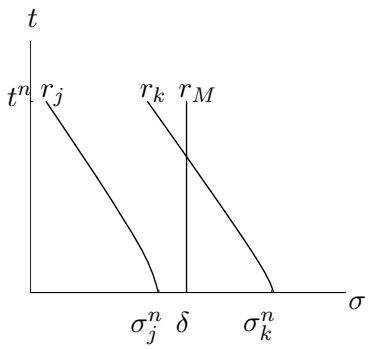

Figure 2: The characteristics through (r_j, t^n) and (r_k, t^n)

The location $\zeta(r_j, t^n)$ is given by $\zeta(r_j, t^n) = \zeta(r_j; \sigma_j^n)$. If for some r_k the corresponding $\sigma_k^n < \delta$ it means that the characteristic corresponding to r_k is inside the physical domain. However, if for some r_k the corresponding $\sigma_k^n > \delta$ it means that the characteristic corresponding to r_k crossed the line $r = \delta$ and σ_k^n is outside the physical domain. Then $\zeta(r_j, t^n) = \zeta(r_j; \sigma_j^n)$ does not correspond to a physical situation anymore. In addition, for all n, when $\sigma_j^n > \delta$ the location of the flame front satisfies $\zeta(r_j, t^n) < \zeta(r_j, t^{n-1})$. Together with the initial condition, this observation implies that when $\sigma_j^n > \delta$ the flame is either in the tube or the flame will enter the tube at a following time level.

To prevent the flame from entering into the tube and to stabilise the flame we will impose the

following rule (stabilisation procedure) P:

$$\begin{aligned} &\text{for all} \quad n \\ &\quad \text{if} \quad \sigma_k^n < \delta \\ &\qquad \zeta(r_j, t^n) = \zeta(r_j; \sigma_j^n), \\ &\quad \text{else} \\ &\qquad \zeta(r_k, t^n) = \zeta(r_k; \delta). \end{aligned} \tag{5.2}$$

From a geometrical viewpoint the procedure P means to cut off the characteristics with the straight line passing through the points $(\delta, 0)$, (δ, t^n), (Figure 2) and to employ only those characteristics that are inside the domain $[0, \delta] \times [0, t^n]$.

The procedure P implies that the flame is fixed above the burner. Indeed, without the stabilisation procedure we would have $\zeta(\delta, t^n) = \zeta(r_M; \sigma_M^n)$. Since $\delta = r_M < \sigma_M^n$, by applying P and by taking into account the initial condition $z_0(\sigma) = 0$ we conclude that $\zeta(\delta, t^n) = \zeta(\delta; \delta) = 0$ for $n = 0, \ldots, N$. This means that the flame is fixed at the point where the laminar burning velocity is equal to the flow velocity. Therefore, P implies the boundary condition $\zeta(\delta, t) = 0$ for $t \geq 0$.

Remark 5.1 *The stabilisation procedure P can also be applied when the initial condition $z_0 \neq 0$, $z_0(\delta) = 0$ provided that the corresponding Jacobian does not vanish. Note that the attachment of the flame at the burner rim will be also implied in this case by P.*

An illustration of some transient flame positions obtained by applying (5.2) to the solution of G-equation for a Poiseulle flow and a constant S_{L} is given in Figure 3.

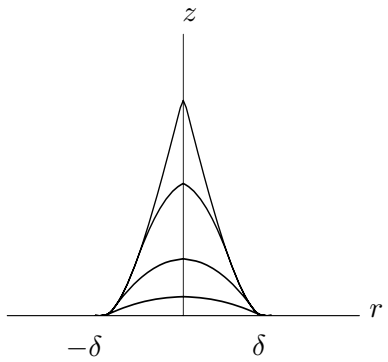

Figure 3: Transient Bunsen flame reaching its stationary position. The intermediary positions depicted here are for values $\hat{t} \in \{0.0333,\ 0.1,\ 0.233,\ 1\}$ and $\hat{v} = 5$.

By applying (5.2) the flame reaches a stationary position equal to $\zeta(r; \delta)$. Thus, from (4.13) the stationary position of the flame $\zeta_{\mathrm{s}}(r)$ is given by

$$\zeta_s(r) = \frac{\delta}{3\lambda}\left(2\hat{v}\mathcal{E}(\alpha, \beta(r), \lambda) - 2\mathcal{F}(\alpha, \beta(r), \lambda) - (\hat{v} - 1)\sin\beta(r)\cos\beta(r)\sqrt{1 - \lambda^2 \sin^2\beta(r)}\right). \tag{5.3}$$

Here the variables α, β and λ are given by

$$\alpha = \frac{\pi}{2}, \quad \beta(r) = \arcsin\left(\frac{r}{\delta}\right), \quad \lambda = \frac{\delta}{\sqrt{1 + \hat{v}^{-1}}}. \tag{5.4}$$

It can be easily shown that the stationary position $\zeta_{\mathrm{s}}(r)$ is equal to the steady state solution of (2.5) subject to the boundary condition $\zeta_0(\delta) = 0$. This steady state solution has the following expression

$$\zeta_0(r) = \int_r^\delta \sqrt{\hat{v}^2(1 - x^2)^2 - 1}\ \mathrm{d}x, \tag{5.5}$$

with δ given in (5.1). By expressing (5.5) in terms of elliptic integrals relation (5.3) is recovered.

The tip of the calculated flame is a cusp whereas the tip of the experimental stationary flame is rounded. In order to obtain a rounded tip for the stationary solution of the G-equation the dependency of S_{L} on the curvature of the flame front needs to be taken into account as computed analytically for the steady G-equation by Peters (2000). To include the curvature effect the G-equation requires a numerical solution method.

The dependency of the flame height $h_{\mathrm{f}} := \zeta_0(0)$ on the dimensionless parameter $\hat{v}$ follows from (5.3) i.e.,

$$h_{\mathrm{f}}(\hat{v}) = \frac{2}{3}\sqrt{\frac{\hat{v}+1}{\hat{v}}}\left(\hat{v}E\left(\sqrt{\frac{\hat{v}-1}{\hat{v}+1}}\right) - K\left(\sqrt{\frac{\hat{v}-1}{\hat{v}+1}}\right)\right). \tag{5.6}$$

In Figure 4 the dependence of the flame height on $\hat{v}$ is depicted. The height of the calculated stationary position of the flame is slightly larger than the experimental one as was compared in (Lewis & von Elbe (1961)).

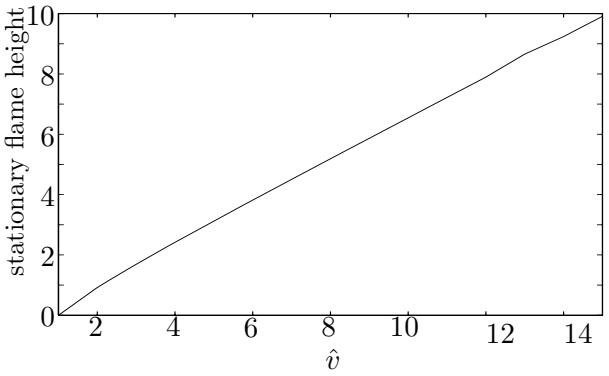

Figure 4: The dependency of the flame height on the dimensionless parameter $\hat{v}$.

6. Stabilisation time

By applying the stabilisation procedure the flame reaches a stationary position after a finite time. We define the moment in time at which the flame reaches its stationary position as the *stabilisation time* of the flame. The nondimensional stabilisation time t_{s} is the smallest time t such that the characteristic through $(0,t)$ crosses the line $r = \delta$. We will show below that the nondimensional stabilisation time t_{s} is approximately 1 independently of the parameter $\hat{v}$. In studying the properties of the stabilisation time we shall need the following lemma.

Lemma 6.1 *The function*

$$f(r) := -\frac{1-r^2}{\sqrt{2(1+r^2)}}K(r) + \sqrt{\frac{2}{1+r^2}}E(r), \tag{6.1}$$

is strictly decreasing from $[0,1]$ *onto* $[1, \frac{\pi}{2\sqrt{2}}]$.

Proof To prove this lemma we will need the following limiting values for complete elliptic inte-

grals (Byrd & Friedman (1971)),

$$\lim_{r\to 0, r>0} \frac{K(r)-E(r)}{r^2} = \frac{\pi}{4}, \tag{6.2a}$$

$$\lim_{r\to 1, r<1} \left(K - \ln \frac{4}{1-r^2} \right) = 0. \tag{6.2b}$$

By using the expressions of the derivatives with respect to the modulus of the complete elliptic integrals (Byrd & Friedman (1971)) the derivative $f'(r)$ becomes

$$f'(r) = \frac{(1-r^2)(E(r)-K(r))}{\sqrt{2}r(1+r^2)^{3/2}}. \tag{6.3}$$

Using (6.2a) follows that $\lim_{r\to 0, r>0} f'(r) = 0$. E is strictly decreasing from $[0,1]$ onto $[1,\pi/2]$ and K is strictly increasing from $[0,1]$ onto $[\pi/2,\infty)$; see (Byrd & Friedman (1971)). Then $f'(r) < 0$ for $0 < r \leq 1$. Thus for $0 \leq r \leq 1$, $\lim_{r\to 1, r<1} f(r) \leq f(r) \leq f(0)$. From (6.2b) and l'Hôspital's rule follows that $\lim_{r\to 1, r<1} f(r) = 1$. Finally, it's easy to see that $f(0) = \pi/2\sqrt{2} = 1.1107$. ∎

Figure 5 shows the graph of f as a function of r.

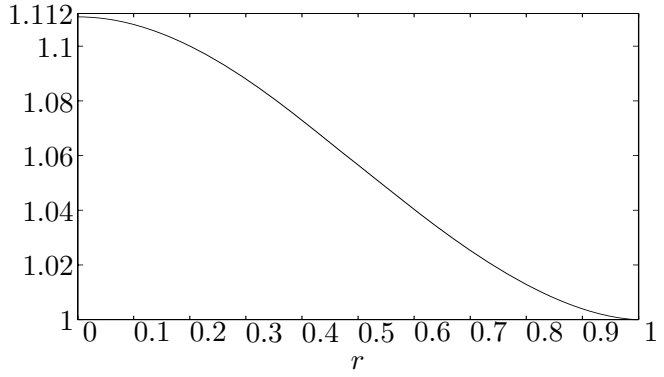

Figure 5: $f(r)$, $0 \leq r \leq 1$

The expression for the nondimensional stabilisation time t_s is given by relation (4.10) i.e.

$$t_s = t(0;\delta). \tag{6.4}$$

For the special case that we study, i.e. $z_0(r) = 0$ the stabilisation time t_s becomes

$$t_s = -\frac{1}{\sqrt{\hat{v}(\hat{v}+1)}} K\left(\sqrt{\frac{\hat{v}-1}{\hat{v}+1}}\right) + \sqrt{\frac{\hat{v}+1}{\hat{v}}} E\left(\sqrt{\frac{\hat{v}-1}{\hat{v}+1}}\right). \tag{6.5}$$

Then $t_s = f(\sqrt{\frac{\hat{v}-1}{\hat{v}+1}})$. Using Lemma 6.1 and taking into account that $\hat{v} \in [2,10]$ follows that $1 \leq t_s \leq 1.0439$. Thus, we can consider that the nondimensional stabilisation time is $t_s \approx 1$.

According to (4.2) the time required for the stabilisation of the flame is directly proportional the radius of the tube and inversely proportional the laminar burning speed S_L. The dependency of the stabilisation time on S_L for a burner with radius 1cm is depicted in Figure 6 (a). As expected the stabilisation time decreases with the laminar burning speed S_L. Figure 6 (b) depicts the dependency of the stabilisation time on the radius of the tube for various values of S_L.

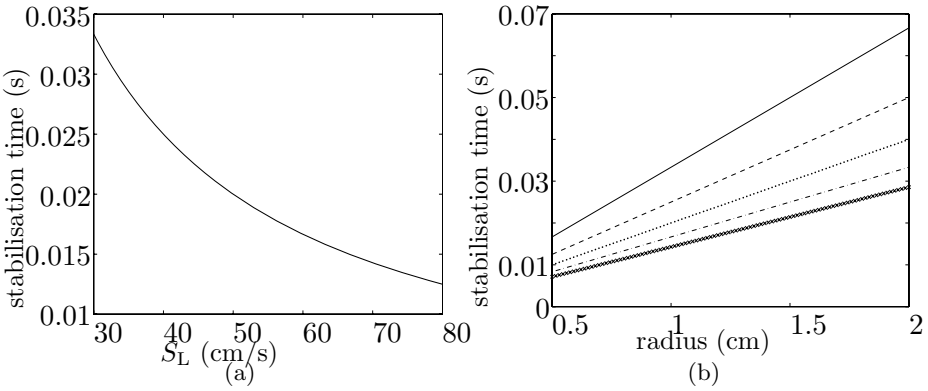

Figure 6: (a) the dependency of the stabilisation time on the laminar burning velocity for a burner with radius 1cm. (b) the dependency of the stabilisation time on the radius of the tube for values of S_L=30cm/s $(-)$, S_L=40cm/s $(--)$, S_L=50cm/s $(\cdots)$, S_L=60cm/s $(-\cdot)$ S_L=70cm/s $(+)$.

7. Stability of the steady state solution

A small perturbation of the front of a stabilised Bunsen flame vanishes in time and the flame recovers its stationary position. In the following we will prove that this real flame feature is captured by our model. In Section 6 we proved that by applying the stabilisation procedure P, the flame reaches a stationary position equal to the steady state solution $\zeta_0(r)$ of the G-equation subject to the boundary condition $\zeta_0(\delta) = 0$. In this section we will show that the steady state solution is stable with respect to the stabilisation procedure P. For this we introduce the following definition.

Definition 7.1 *The steady state solution $\zeta_0(r)$ of the G-equation is said to be stable with respect to stabilisation procedure P if for any small perturbation $\varepsilon(r) \in C^1([0,\delta])$ with $\varepsilon'(r)$ small the solution $\zeta^\varepsilon(r,t)$ of the G-equation with the initial condition $\zeta_0(r)+\varepsilon(r)$ together with the stabilisation procedure P, approaches the steady state solution $\zeta_0(r)$ of the G-equation in the limit of $|\varepsilon(r)|$ and $|\varepsilon'(r)|$ tending to zero.*

In the following we will provide arguments to show that $\zeta_0(r)$ is stable in the sense of Definition 7.1. Let us consider a perturbation $\varepsilon(r)$ such that $|\varepsilon(r)|$ and $|\varepsilon'(r)|$ are small. To find the solution of the G-equation with the initial condition $\zeta_0^\varepsilon(r) := \zeta_0(r)+\varepsilon(r)$ we apply the method of characteristics (see Section 3 and Section 4). For $\sigma \in (0,\delta] \cup [\sqrt{1+\hat{v}^{-1}}, \infty)$ the solution $\zeta^\varepsilon(r;\sigma)$ along the characteristics is given in (4.13) in which $z_0^\varepsilon(\sigma) := \zeta_0(\sigma)+\varepsilon(\sigma)$ replaces $z_0(\sigma)$ and $c^\varepsilon(\sigma) := \sqrt{1+(\zeta_0'(\sigma)+\varepsilon'(\sigma))^2}+\hat{v}\sigma^2$ replaces $c(\sigma)$. We proved in Section 6 that by applying the stabilisation procedure the solution of the G-equation approaches at finite time $t_s = t(0;\delta)$ the stationary position $\zeta_s(r) = \zeta(r;\delta)$. Thus, by applying the stabilisation procedure to ζ^ε it will reach at finite time $t_s^\varepsilon := t^\varepsilon(0;\delta)$ the stationary position $\zeta_s^\varepsilon(r) := \zeta^\varepsilon(r;\delta)$. Then, to prove stability it is enough to prove that $\zeta_s^\varepsilon \approx \zeta_s$ when $|\varepsilon(r)|$ and $|\varepsilon'(r)|$ are small. For $|\varepsilon'(r)|$ small $c^\varepsilon(\delta) = \sqrt{1+(\varepsilon'(\delta))^2}+\hat{v}-1 \approx c(\delta)$. Using continuity of the elliptic integrals with respect to the modulus and the argument (Byrd & Friedman (1971)) and taking into account that $\zeta_0^\varepsilon(\delta) = 0$ it follows that $\zeta^\varepsilon(r;\delta) \approx \zeta(r;\delta) = \zeta_0(r)$. Thus, we can conclude that the steady solution of the G-equation is stable with respect to the stabilisation procedure P.

8. Conclusion

The propagation of a Bunsen flame from a flame kernel to a stationary position is investigated by employing a kinematic model based on the G-eqation. The analysis included in this paper shows that with the kinematic model only it is not possible to chapture the flame stabilisation. This paper proposes an improved kinematic model that accounts for the flame stabilisation. The improvement is based on a correlation between mathematical and physical observations. In addition, the relation between the position of the characteristics corresponding to the G-equation with respect to the physical domain and the location of the flame front is analysed. Based on this analysis a mathematical rule that allows for flame stabilisation is derived. To assess the flame front dynamics we solved the G-equation analytically using the method of characteristics. This allows us to derive analytic expressions in terms elliptic integrals of first and second type for the location of the characteristics, location of the flame front along the characteristics and for the stationary position of the flame front. The stationary position of the flame is shown to be equal to the steady state solution of the G-equation. The flame obtained with the improved kinematic model captures features of real flames i.e., the stationary position is stable with respect to small perturbation of the flame front and the stabilisation time is proportional the ratio between the tube radius and the laminar speed. These results will give further insights in the behaviour of flame dynamics for more complex situations, that will be investigated next.

9. Acknowledgements

The authors would like to thank Dr. K. Schreel and Dr. S. Pop for useful discussion. This research is supported by the Technology Foundation STW, applied science division of NWO and the technology programme of the Ministry of Economic Affairs, project number EWO.5646.

References

Abramowitz, M. & Stegun, I. (1974) *Handbook of mathematical functions, with formulas, graphs, and mathematical tables.* Dover Publications

Boyer, L. & Quinard, J. (1990) On the dynamics of anchored flames, *Combust. Flame,* **82** , 51–65.

Byrd, P.F. & Friedman, M.D. (1971) *Handbook of elliptic integrals for engineers and scientists.* Berlin. Göttingen. Heidelberg:Springer-Verlag

Carlson, B.C. & Notis, M. (1991) Algorithms for Incomplete Elliptic Integrals [S21] , *ACM T. Math. Software,* **7**

Carlson, B.C. (1979) Computing elliptic integrals by duplications, *Num. Math.,* **33**, 1–16

Dowling, A.P. (1999) A kinematic model of a ducted flame, *J. Fluid. Mech.,* **394**, 51–72

Ducruix, S., Durox, D. & Candel, S. (2000) Theoretical and experimental determination of the transfer function of a laminar premixed flame , *P. Combust. Inst.,* **28**, 756–773

Fleifil, M., Annaswamy, A.M., Ghoneim, Z.A., & Ghoniem, A.F. (1996) Response of a laminar premixed flame to flow oscillations: A kinematic model and thermoacustic instability results , *Combust. Flame,* **106**, 487–510

Kevorkian, J. (1990) *Partial Differential Equations. Analytical Solution Techniques.* NewYork.London:Chapman and Hall

Lewis, B & Elbe, G (1961) *Combustion, Flames and Explosions of Gases* New York.London:Academic Press Inc.

Lieuwen, T. (2003) Acoustic near-field characteristics of a conical, premixed flame, *J. Acoust. Soc. Am.,* **113**, 167–177

Lieuwen, T. (2005) Nonlinear kinematic response of premixed flames to harmonic velocity disturbances, *P. Combust. Inst.,* **30**, 1725–1732

Markstein, H.G. (1964) *Nonsteady flame propagation.* Oxford:Pergamon Press

Peters, N (2000) *Turbulent Combustion.* Cambridge Monographs on Mechanics